Chapter 2

Acoustic Emission to Detect Damage in FRP Strength Under Freeze and Thaw Cycles

Hyun-Do Yun and Wonchang Choi

Additional information is available at the end of the chapter

http://dx.doi.org/10.5772/53813

1. Introduction

Strengthening with carbon fiber reinforced polymer (CFRP) sheets and plates, as opposed to the use of steel plates, has been employed recently in the rehabilitation and retrofitting of infrastructures due to better performance (than that of steel plates) in terms of resistance to corrosion and high stiffness-to-weight ratios. Because concrete structures are exposed periodically to snow and freezing temperatures during the winter season, a reduction in structural integrity, such as observed in the deterioration of the concrete and the degradation of the FRP bond system, is evident in field conditions. In terms of environmental exposure, periodic temperature changes such as freeze and thaw cycles can cause devastating damage to RC structures.

Since 1989, research by Kaiser [1] has been used to investigate the structural integrity of CFRP-strengthened RC beams exposed to freeze and thaw cycling. Results indicate that the strength of RC beams with CFRP sheets does not decrease with fewer than 100 cycles ranging from -25°C to 25°C. Similar test results are reported by Baumert and Bisby [2] who conducted tests on CFRP-strengthened RC beams exposed to temperatures ranging from -27°C to 21°C and from -18°C to 15°C with 50 freeze and thaw cycles for each temperature. Bisby and Green [3] examined the bonding performance of concrete members strengthened with CFRP and glass FRP under freeze and thaw cycling with temperatures ranging from -18°C to 15°C. Their results indicate insignificant effects on strengthening in flexure within 300 cycles of freeze and thawing. The American Concrete Institute (ACI) 440R-02 [4] recommends that the FRP system, which is exposed to high humidity, freeze-thaw cycles, salt water, or alkalinity, should be taken into account when determining the environmental degradation of an adhesively bonded system.

2. Problem statement

Because the condition of strengthened concrete is not visible from outside the CFRP sheets, it is difficult to quantify the deterioration and any defects that affect the structural integrity of the infrastructure. Evaluation techniques are needed to expand CFRP's application in repair and rehabilitation. With that need in mind, an acoustic emission technique is employed to determine the performance of CFRP-strengthened RC beams exposed to freeze and thaw cycling.

The author's previous study successfully shows the possible application of acoustic emission activities to determine the structural integrity corresponding to the representative damage levels of CFRP-strengthened RC beams that contain intentional defects in the bond system [5]. In this research, the acoustic emission signal characteristics of RC beams strengthened with CFRP sheets and exposed to several freeze and thaw cycles (0, 30, 60,120, and 400 cycles) ranging in temperature from -18 to 4°C are investigated.

For this study, six beams were fabricated in 100 x 100 x 400 mm sections with a specified design compressive strength of 33 MPa for all specimens. The specimens were designed in shear failure regardless of the shear reinforcement with CFRP. Specimen S1 indicates the control beam without any strengthening or freeze and thaw cycles. Specimens S2 indicate the shear-strengthened beams with CFRP sheets (0.12 mm thickness). Detailed reinforcement and specimen information is presented in Figure 1.

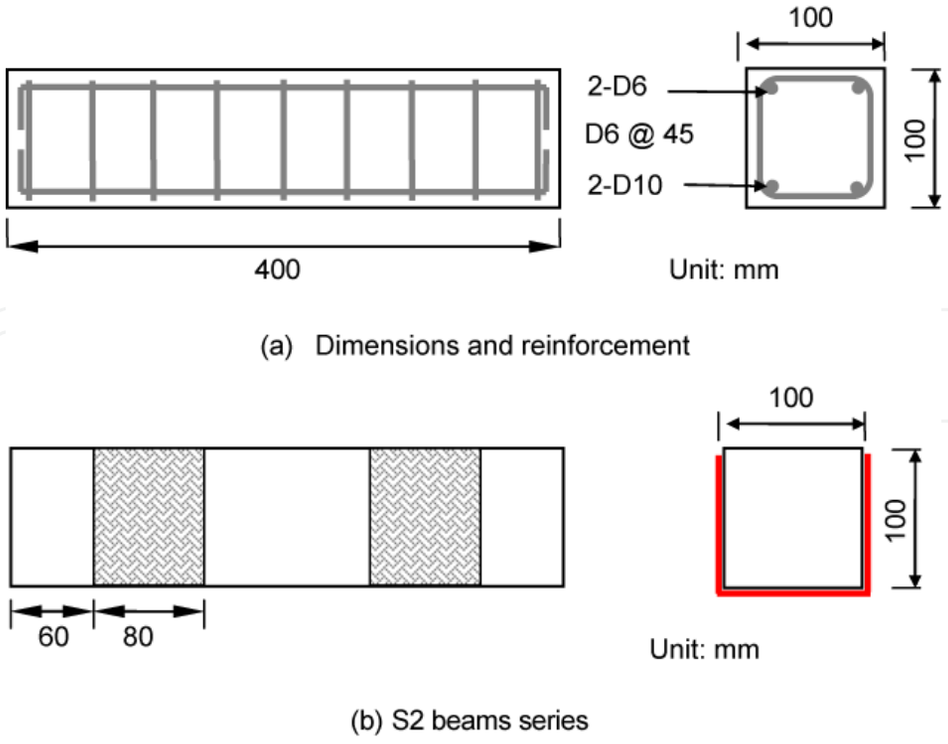

Figure 1. Detailed information regarding the test specimens

http://dx.doi.org/10.5772/53813

The CFRP sheets used in this study have tensile strengths of 4,100 MPa, respectively. The adhesive (Sikadur-330) used for bonding the CFRP composites is epoxy resin, and its bonding strength, as supplied by the manufacturer, is 17.5 MPa. The material properties of the reinforcement in the specimens are listed in Table 1.

	Size of Rebar (diameter, area)	Yielding Strength (MPa)	Yielding Strain (μm)
Longitudinal Reinforcement	D13 (12.7mm, 1.267cm^2)	255	2130
Transverse Reinforcement	D6 (6.35mm, 0.3167cm^2)	290	1920
Compression Reinforcement	D6 (6.35mm, 0.3167cm^2)	290	1920

Table 1. Material Properties of Reinforcement

The simply supported specimens were tested under four-point loading conditions by a 2000 kN Universal Testing Machine (UTM). The load was applied up to failure with displacement control of 0.1 mm/sec. Figure 2 shows the typical test set-up for the specimens used in this study. A linear variable differential transducer (LVDT) was installed to measure the displacement at the mid-span of the specimen. An electrical strain gauge also was installed to measure the strain in the tensile reinforcement and concrete. Four acoustic emission sensors (Model SE900-MWB with wide bandwidth) with a frequency range of 100~ 900 kHz were installed to measure the acoustic emission activities that correspond to the damage level of the specimens under flexure. These sensors were pre-amplified (at 20 dB) prior to recording in order to prevent noise signals due to friction, and a rubber sheet was placed between the beam and loading points. The threshold level was fixed to 35 dB to eliminate electric and mechanical noise. The acoustic emission signals were recorded up to the failure of the specimens.

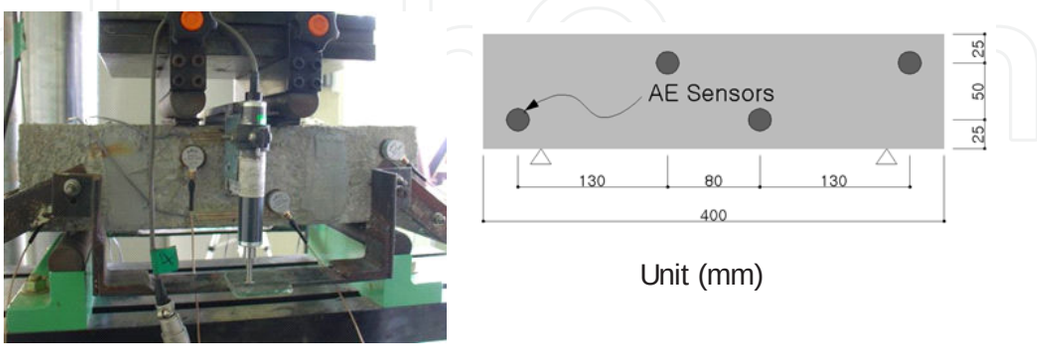

Figure 2. Typical test set-up and gauge installation

As the diagonal crack width expands, the specimen fails in shear mode, while multiple flexural cracks were generated for the S2 specimens with CFRP strengthening. For specimen

S1, the flexural crack initiates at the mid-span of the specimen around 12% (12 kN) of the ultimate strength, and then diagonal cracking is generated at around 30% (29kN) of the ultimate strength. As the diagonal crack width expands, the specimen fails in shear mode, while multiple flexural cracks were generated for the S2 specimens with CFRP strengthening.

As the load increases, the diagonal crack width increases, and then finally it fails in shear mode. Similar crack propagation was observed for all CFRP-strengthened specimens. As seen in Figure 3, the CFRP-strengthened specimens exposed freeze and thawing cycles partially de-bonded due to the deterioration of the interface between the concrete surface and adhesive.

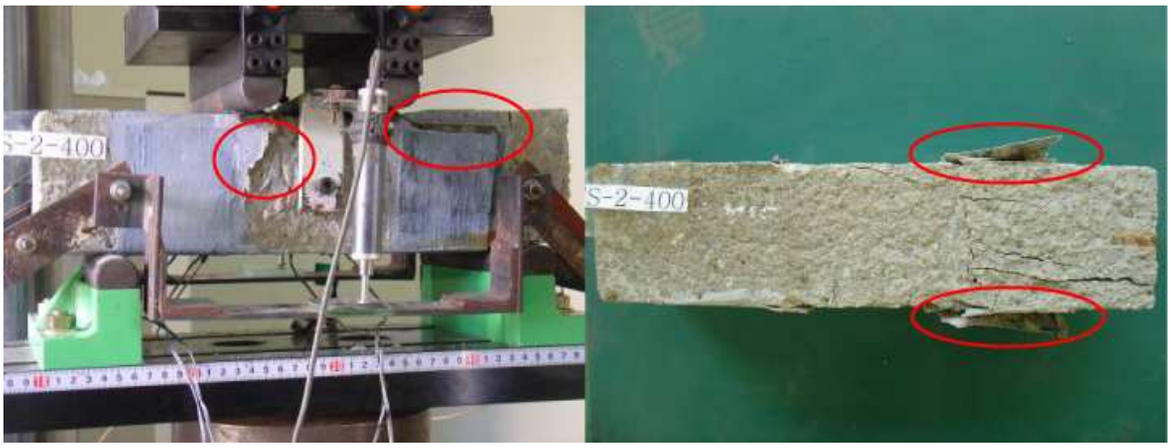

Figure 3. De-lamination of CFRP at failure

Figure 4 shows the load versus displacement relationship of the specimens. The CFRP-strengthened specimens prevent rapid strength reduction due to diagonal cracking once the ultimate strength is attained. The strength and ductility tend to decrease for the CFRP-strengthened specimens over 60 freeze and thawing cycles.

For the CFRP-strengthened specimen, the deformation in the diagonal direction rapidly increases. This occurrence results in the shear strengthening of the CFRP sheets. Moreover, the deformation in the diagonal direction increases as the number of freeze and thawing cycles increases. This occurrence results in the reduction of bond strength between the concrete surface and CFRP sheets.

2.1. Acoustic emission activities

2.1.1. Event counts and energy

Figure 5 shows the relationship between acoustic emission event counts and energy that corresponds to the normalized elapsed time (T/T_u). The normalized elapsed time is computed using the ratio of the loading time (T) to the moment of failure (T_u). The moment of failure is determined at the time of 80% ultimate strength after reaching the ultimate strength. Figure 5 show the rapid increase in the acoustic emission event counts at the initiation of flexural

http://dx.doi.org/10.5772/53813

cracking. No external cracks or visible damage are evident prior to the initiation of the flexural cracks; however, a low level of events was recorded, which is possibly due to the voids and micro-cracks within the concrete.

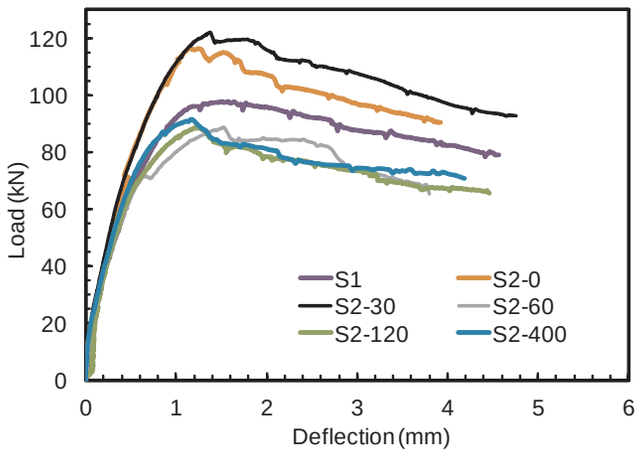

Figure 4. Load versus displacement

For specimen S1, the acoustic emission event counts moderately increase after the initiation of the flexural cracks.

For specimen S2, the acoustic emission event counts moderately increase after the initiation of the flexural cracks. Otherwise, the acoustic emission event counts for the CFRP-strengthened specimen, S2, increase and continue to increase along with the damage of adhesion in the interface between the concrete and CFRP plates.

The acoustic emission event counts for specimen S1 at the normalized elapsed time ratio of 41% drop within a short period due to the occurrence of diagonal cracks. Subsequently, the acoustic emission event counts increase up to the normalized elapsed time ratio of 64%, which is due to the incremental growth of the width of the existing diagonal crack, instead of the occurrence of a new crack. Compared with the occurrence of new cracks, increasing the width of existing cracks may result in a decrease in the occurrence of elastic waves [5].

Figure 5 show that the acoustic emission event counts for the specimens exposed to freeze and thaw cycles gradually increase from the beginning of the loading and continue to increase up to the ultimate loading. This occurrence may result in the weakness of the bond strength of the concrete within that causes deterioration of the structural integrity of the RC member. The acoustic emission energy tends to decrease gradually with an increase in the number of freeze and thaw cycles as shown in Figure 5.

The AE energy can be evaluated by the area of AE elastic waves. The AE energy level of the strengthened beam is higher energy level than that of the beam without strengthening. This was because the amplitude of AE signal due to the damage of epoxy is greater than that due to the crack in the concrete beam. The AE energy over 30 freeze and thawing cycles was rapidly increased. This was because the emitted AE elastic waves from the reduced bonding

force between the CFRP sheets and epoxy were relatively lower than that from the rupture of epoxy which typically has a high level of amplitude characteristic.

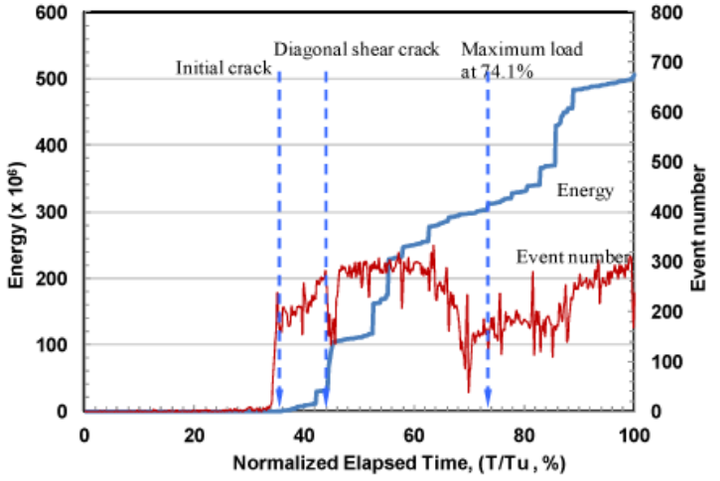

(a) S1 (without strengthening, and freeze and thaw)

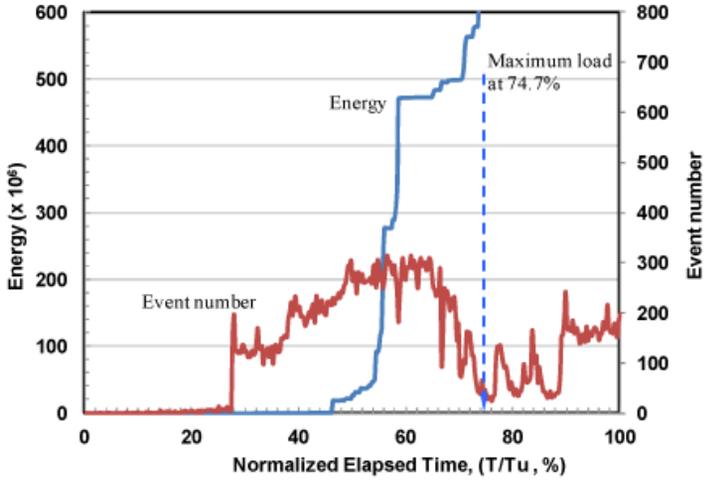

(b) S2-0 (without free and thawing)

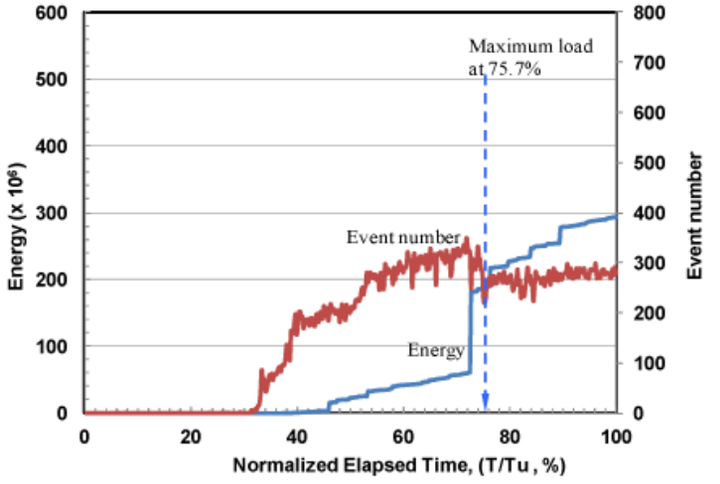

(c) S2-30

http://dx.doi.org/10.5772/53813

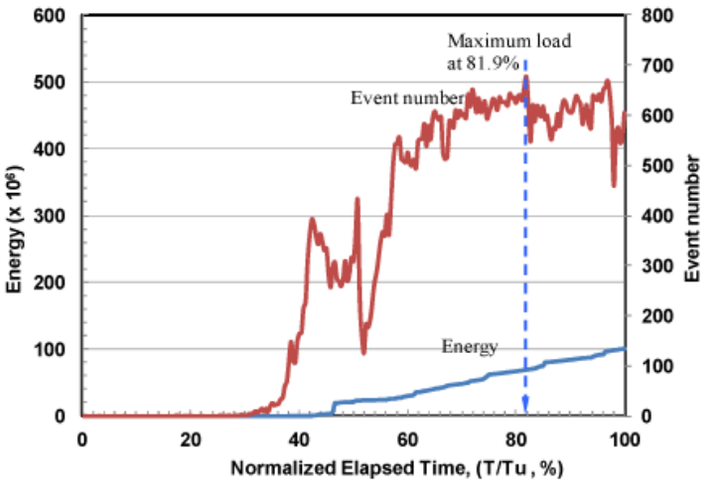

(d) S2-60

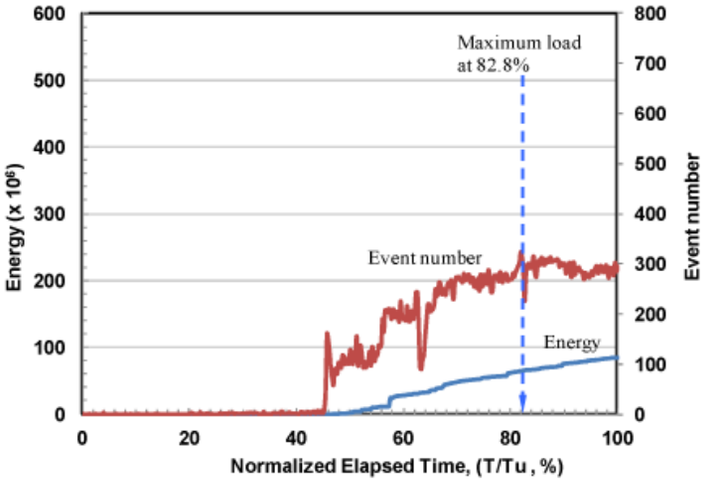

(e) S2-120

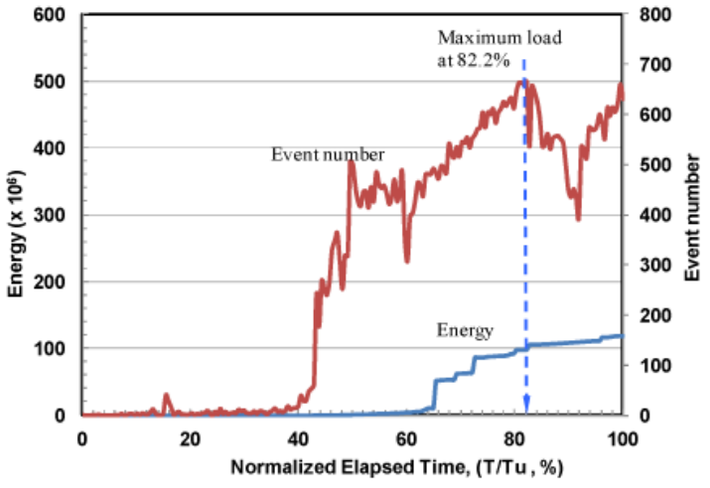

(f) S2-400

Figure 5. Acoustic emission event counts and energy characteristics of RC beams with CFRP composites (up to $0.80P_{max}$ after maximum loading)

2.2. Amplitude and frequency

Figure 6 shows the progress of amplitude and frequency that corresponds to the normalized loading ratio for selected specimens. The amplitude and frequency of specimen S1 increase considerably from the beginning of the load to the initial flexural crack, as shown in Figure 6 (a). This result is caused by the development of macro-cracks that represent the connection of the voids and entrapped air within the concrete. The incremental development of the macro-cracks continues until diagonal cracks begin to appear. The frequency decreases radically once these diagonal cracks appear. However, the amplitude does not change significantly. The frequency decreases continuously until the ultimate load is reached. Afterward, it is in the range of 100 – 200 kHz until failure.

For specimen S2, the acoustic emission signal is detected at the beginning of loading. Specimen S2 generates a higher amplitude and frequency than specimen S1. These higher acoustic emission signals might be caused by the damage of epoxy on the concrete surface and CFRP plate. No considerable change is evident from the beginning of the de-bonding of the CFRP to the ultimate loading and failure. The frequency until failure is in the range of 150 – 250 kHz, which is a higher frequency than for specimen S1. This finding is due to the acoustic emission signal characteristics of the epoxy in the interface between the concrete and CFRP sheets.

On the other hand, specimens S2-120 and S2-400 generate low amplitude and frequency at the initial flexural cracks and diagonal cracks. This occurrence results in the deterioration of the epoxy and/or the concrete surface due to the considerable number of freeze and thawing cycles.

As shown in Figure 8 (f), the more freeze and thawing cycles, the more deterioration of the concrete surface and CFRP sheets. This deterioration results in the significant increase in amplitude and frequency during the beginning of loading up to the de-bonding of the CFRP. Afterward, the acoustic emission signal decreases. The frequency until failure is in the range of 200 – 350 kHz, which is a relatively high frequency range. In general, there is a tendency for the amplitude and frequency to increase as the micro-cracks and initial flexural cracks develop. The frequency tends to decrease as the diagonal cracks propagate and the crack widths expand, although the maximum amplitude does not change.

2.3. Damage evaluation

In order to apply acoustic emission techniques to the evaluation of damage and integrity of CFRP-strengthened RC beams, it is essential to study the characteristics of the acoustic emission parameters according to damage levels. The evolution of acoustic activity caused by micro-fracture within the concrete is often quantified using the concise framework originated by Gutenberg and Richter in their analysis of earthquake magnitudes, which is a reflection of the view that large-scale (i.e., geological) and small-scale (i.e., micro-fracture) acoustic events share a common origin in cascades of strain energy release events. In earthquake seismology, events of larger magnitude occur less frequently than events of smaller

http://dx.doi.org/10.5772/53813

magnitude. This fact can be quantified in terms of a magnitude-frequency relationship, for which Gutenberg and Richter propose the empirical formula (1),

$$\log N(W) = a - bW, \tag{1}$$

where *N(W)* is the Richter magnitude of the events, which is the cumulative number of events having a magnitude greater than or equal to *W*, and a and b are the empirical constants.

In acoustic emission data analysis, the coefficient *b* is known as the AE-b value [6]. The AE-b value is given as the gradient of the linear descending branch of the cumulative frequency distribution. The coefficient 20 was multiplied to get the AE-b values to the slope [7]. In the process where micro-fractures are more prevalent than macro-fractures, the b-value tends to increase, whereas in the process whereby macro-fractures occur more frequently than micro-fractures, the b-value tends to decrease.

Figure 7 presents the relationship of maximum amplitude versus frequency during the specific normalized elapsed time, which indicates the representative damage level. For specimen S2-120, the AE-b value is 1.389 when the micro-cracks initiate on the surface and can be detected visually. As the cracks propagate and expand, the values are 1.222 and 1.051, respectively. Those values tend to decrease as damage progresses. In short, the AE-b values tend to increase when the micro-cracks dominate the overall behavior, whereas the AE-b values seem to decrease when the behavior is controlled primarily by the propagating and expanding cracks [6, 8].

Figure 8 presents the comparison between the AE-b values versus the normalized elapsed time to failure. For specimen S-1, the AE-b value decreases significantly at the initiation of the diagonal cracks and flexural compression failure, at which time considerable damage is generated. This occurrence results in a high acoustic emission signal.

For specimen S-2, the lowest AE-b value is obtained at the de-bonding of the CFRP. Afterward, the rapid decrease in the AE-b value can be observed around the point of failure.

Specimens with fewer than 120 freeze and thawing cycles have relatively higher AE-b values (higher than 1.2) at the initiation of the micro-cracks and diagonal cracks and de-bonding of the CFRP. In general, the AE-b values range from 1.20 to 1.45, which is a relatively narrow fluctuation range compared to that for the specimens that are not exposed to freeze and thawing cycles.

For specimens exposed over 400 freeze and thawing cycles (S2-400), the low AE-b values are obtained at the beginning of the elapsed time, which may result in the deterioration of the concrete surface and bonding surface with the CFRP. The damage level caused by the freeze and thawing cycles is comparable to that of the macro-cracks. This occurrence is caused by the low acoustic emission values at the beginning of the test.

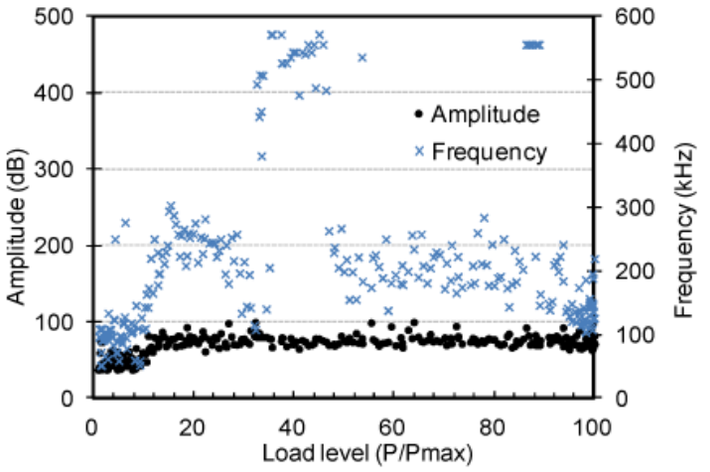

(a) S1 without strengthening, and freeze and thaw

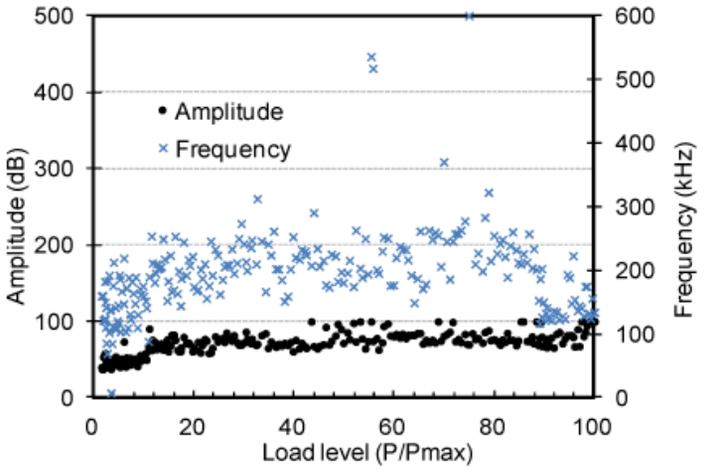

(b) S2 without free and thawing

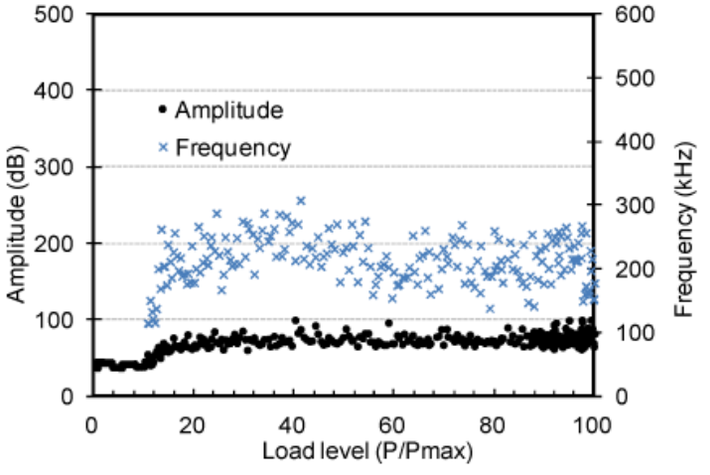

(c) S2-30

http://dx.doi.org/10.5772/53813

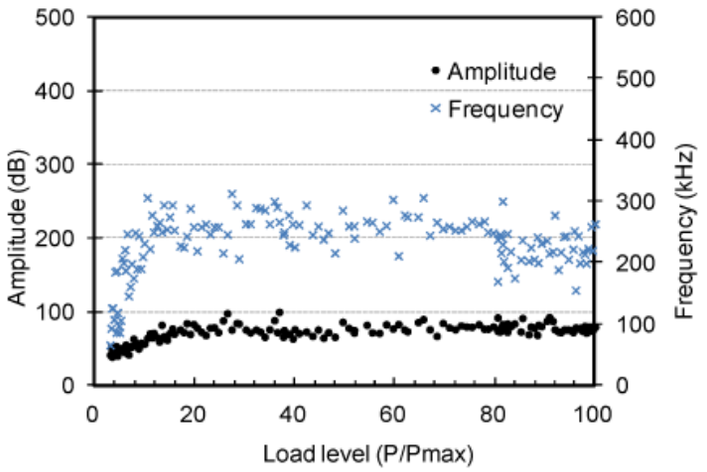

(d) S2-60

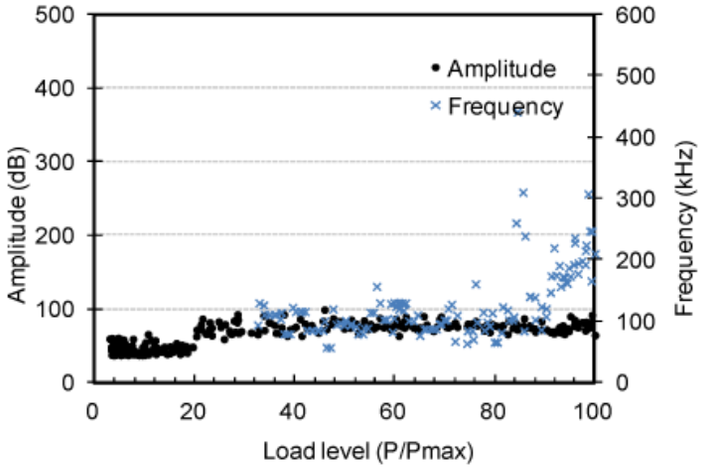

(e) S2-120

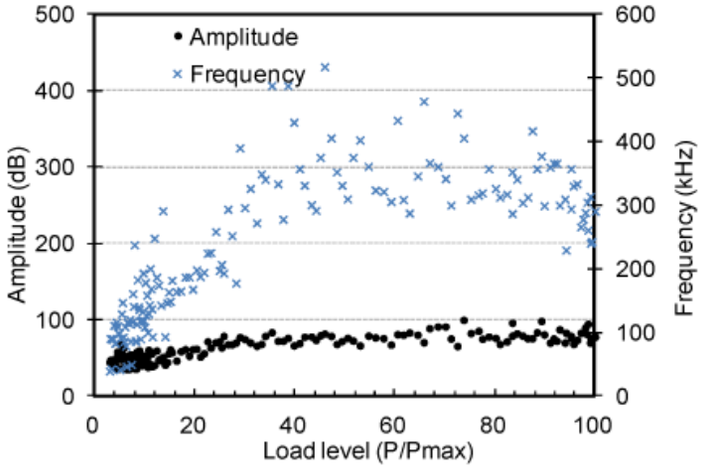

(f) S2-400

Figure 6. Frequency and amplitude

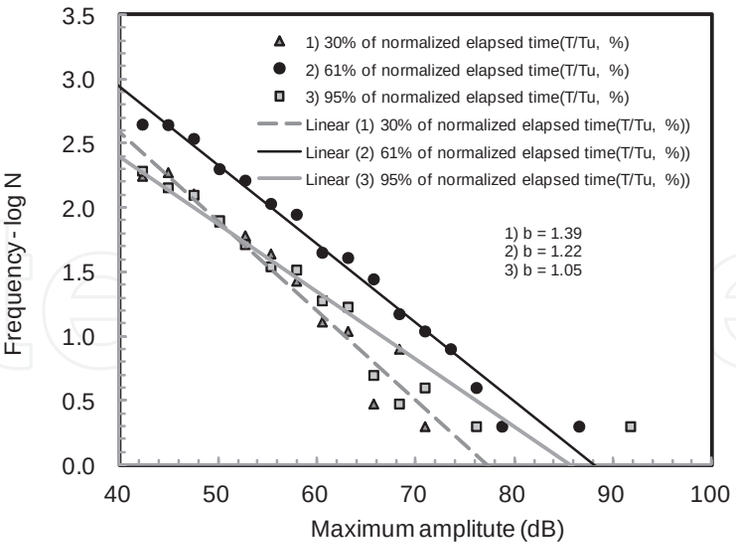

Figure 7. Typical variations of amplitude and load for S2-120

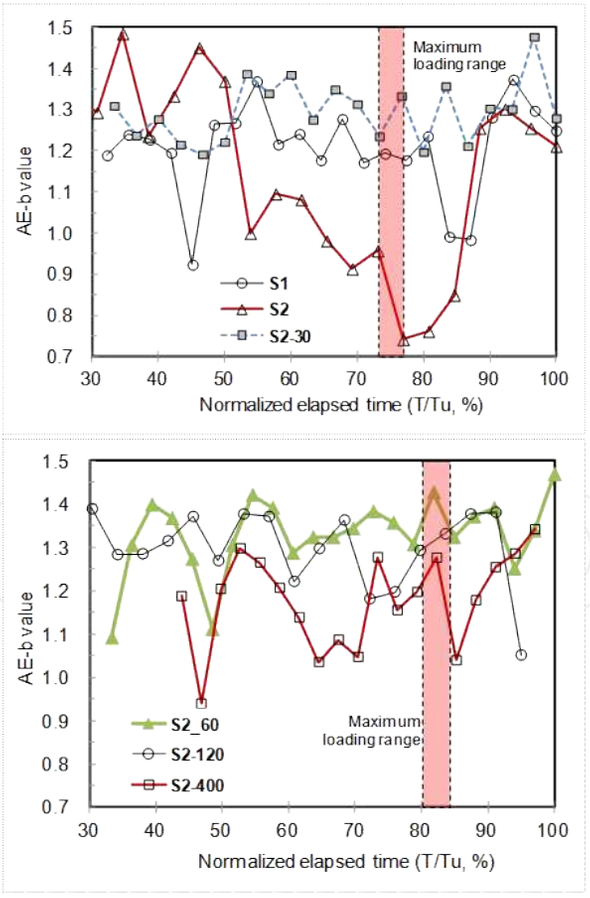

Figure 8. The AE-b values versus the normalized elapsed time to failure

http://dx.doi.org/10.5772/53813

In order to quantify the evolution of the damage process during the loading of the CFRP-strengthened RC beams, the AE-b values are separated into three subpopulations representing each damage level (i. micro cracks; ii. crack propagation and/or crack growth; iii. macro cracks; de-bonding, and/or CFRP failure). The relationship between the physical damage level and the AE-b value is presented in Table 2.

Range of AE-b values	Damage description
AE-b values "/> 1.25	Development of micro-crack
1.25 "/> AE-b values "/> 1.15	Propagation of micro-crack and crack width
1.15 "/> AE-b values "/> 0.80	Formation of macro-crack, de-bonding of CRFP, rupture

Table 2. AE-b Values for Each Damage Level

3. Conclusions

The strengthening performance and evaluation of the damage caused by acoustic emission activities for RC beams strengthened in shear with CFRP are examined under various freezing and thawing cycles with and without shear strengthening. The following results are found based on the limited experimental tests.

The significant increase in acoustic emission activities (event, energy, amplitude, and frequency) is observed at each damage level that corresponds to the initiation of the crack, propagation of diagonal cracking, de-bonding of CFRP, and failure. These acoustic emission activities are good indicators for determining the structural integrity and micro-damage of CFRP-strengthened RC beams.

The AE-b value provides a possible application to quantify the local damage of CFRP-strengthened RC beams exposed to freeze and thaw cycling corresponding to various damage levels.

Author details

Hyun-Do Yun[1] and Wonchang Choi[2]

1 Chung-Nam National University, Korea

2 NC A&T State University, USA

References

[1] Kaiser, H. P. Strengthening of Reinforced Concrete with Epoxy-Bonded Carbon Fibre Plastics. Doctoral thesis. Eidgenossische Technische Hochschule (ETH), Zurich: Switzerland; 1989.

[2] Baumert, M. E., M. F. Green, and M. A. Erki. Proceedings of the Second ACMBS International Conference, August11-14, 1996, Montreal, Canada.

[3] Bisby, L. A. and M. F. Green. Resistance to Freezing and Thawing of Fiber-Reinforced Polymer Concrete Bond. ACI Structural Journal 2002; 99(2) 215-223.

[4] ACI 440. Guide for the Design and Construction of Externally Bonded FRP systems for Strengthening Concrete Structures. 2002.

[5] Yun, H., W. Choi, and S. Seo. Acoustic Emission Activities and Damage Evaluation of Reinforced Concrete Beams Strengthened with CFRP Sheets. NDT & E International, Elsevier, 2010; 43(7) 615-628.

[6] Shitotani, T., Y. Nakanishi, X. Luo, and H. Haya. Damage Assessment in Railway Sub-structures Deteriorated Using Acoustic Emission Technique, DGZFP-Proceedings BB 90-CD, 2004.

[7] K. Mogi, Study shocks caused by the fracture of heterogeneous materials and its relations to earthquake phenomena, Bulletin of Earthquake Research Institute, University of Tokyo,1962; 40 123-173.

[8] Colombo, I. S., I. G. Main, and M. C. Forde. Assessing Damage of Reinforced Concrete Beam Using b-value Analysis of Acoustic Emission Signals. Journal of Materials in Civil Engineering, ASCE, 2003; 15(3) 280-286.